

Supporting Information

Evaluation of Miniaturized Ultrasonic Nebulization for High-efficiency Sampling in Characterization of Silver Nanoparticles by Single Particle Inductively Coupled Plasma Mass Spectrometry

Junhang Dong,^{1,2} Zhenli Zhu^{1,2,3*}, Lujie Li,^{1,2} Pengju Xing¹, Shuyang Li,¹ Lei Ouyang,² Xing Liu,¹ Wei Guo,¹ Hongtao Zheng², and Rong Qian^{4*}.

¹ State Key Laboratory of Biogeology and Environmental Geology, School of Earth Sciences, China University of Geosciences, Wuhan 430074, China

² Faculty of Material Science and Chemistry, China University of Geosciences, Wuhan 430074, China

³ Hubei Key Laboratory of Yangtze Catchment Environmental Aquatic Science, Wuhan, 430078, China

⁴ National Centre for Inorganic Mass Spectrometry in Shanghai, Shanghai Institute of Ceramics, Chinese Academy of Sciences, Shanghai 200050, China

Correspondence and requests for materials should be addressed to:

Dr. Zhenli Zhu, State Key Laboratory of Biogeology and Environmental Geology, China University of Geosciences, Wuhan 430074, China, Email: zlzhu@cug.edu.cn

Dr. Rong Qian, National Centre for Inorganic Mass Spectrometry in Shanghai, Shanghai Institute of Ceramics, Chinese Academy of Sciences, Shanghai 200050, China, Email: qianrong@mail.sic.ac.cn

Table of Contents

Figure S1. Comparison of the pulse signal profiles generated from 100 nm Ag NPs by MUN-spICP-MS and PN-spICP-MS, with the sample uptake flow rate of 10 $\mu\text{L min}^{-1}$ and 346 $\mu\text{L min}^{-1}$, respectively.

Figure S2. The influence of carrier gas flow rate on the TE values and average pulse signal intensity of MUN-spICP-MS.

Figure S3. Pulse signal profiles during the rinsing processes using MUN-spICP-MS (a) with and (b) without EDTA addition. These rinsing processes were conducted after continuous introduction of 60 nm Ag NPs for 5 minutes.

Figure S4. Diameter characterization results of (a) 60 nm and (b) 100 nm Ag NPs using transmission electron microscope (TEM).

Figure S5. Linear correlation analysis between signal intensity and nanoparticle volume for Ag NPs of various sizes, comparing MUN-spICP-MS (red line) and PN-spICP-MS (blue line). The horizontal axis represents nanoparticle volume calculated from NPs diameters, while the vertical axis represents the average signal intensity of NP pulse signals collected over 5 minutes. All intensities were normalized to the maximum value.

Table S1. Driven power of the MUN system at different sample uptake flow rates.

Table S2. The TE of MUN-spICP-MS at different sample uptake flow rates.

Table S3. The comparison between the measured diameters of Ag NPs using MUN-sp-ICPMS, PN-spICP-MS, TEM, alongside the nominal values provided by the supplier.

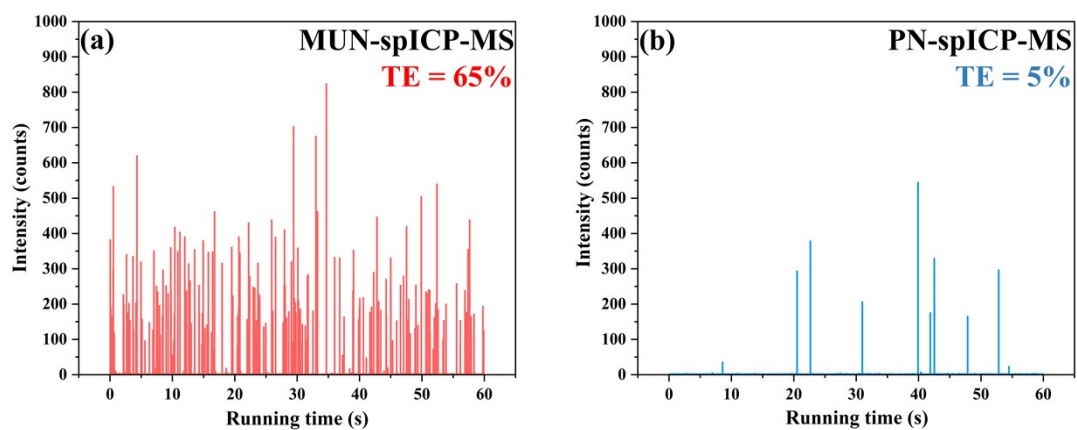


Figure S1. Comparison of pulse signal profiles generated from 100 nm Ag NPs by MUN-spICP-MS and PN-spICP-MS, with the sample uptake flow rate of $10 \mu\text{L min}^{-1}$ and $346 \mu\text{L min}^{-1}$, respectively.

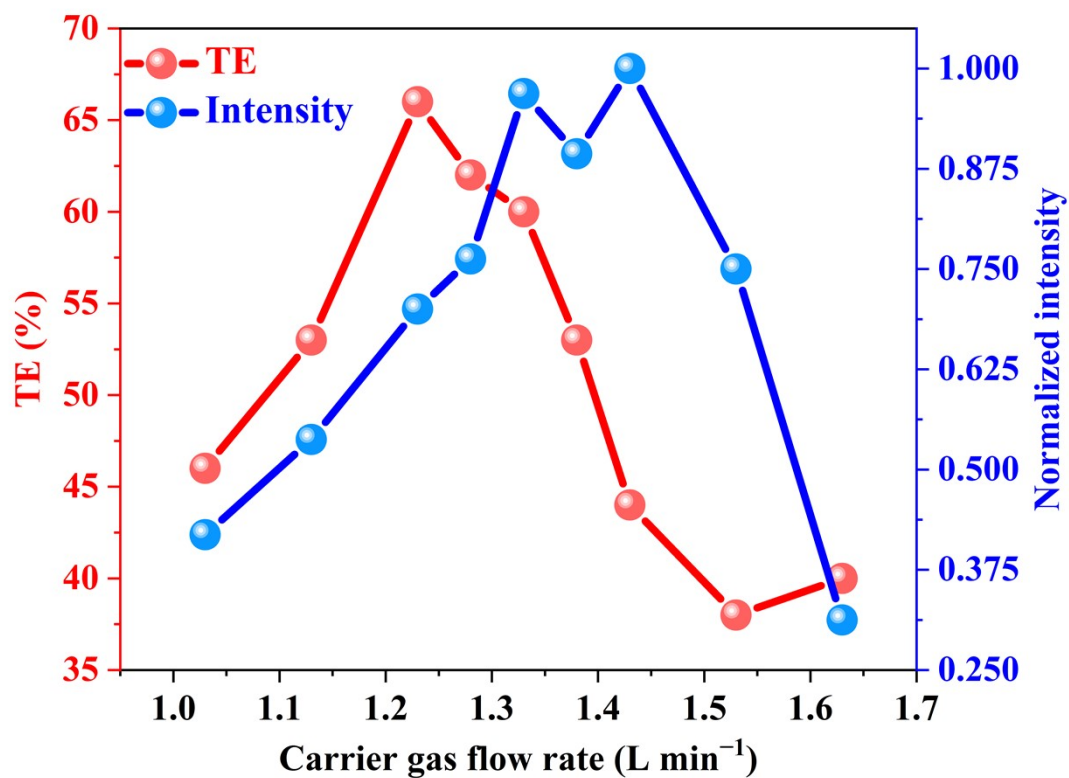


Figure S2. The influence of carrier gas flow rate on the TE values and normalized average pulse signal intensity of MUN-spICP-MS.

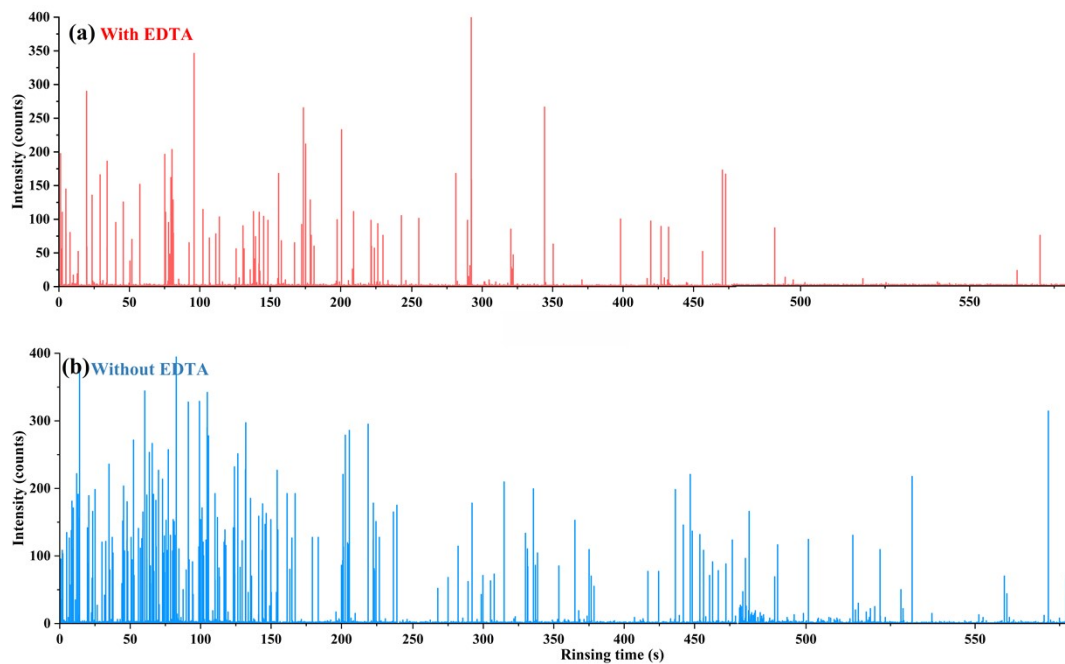


Figure S3. Pulses signal profiles during the rinsing processes using MUN-spICP-MS (a) with and (b) without EDTA addition. These rinsing processes were conducted after the continuous introduction of 60 nm Ag NPs for 5 minutes.

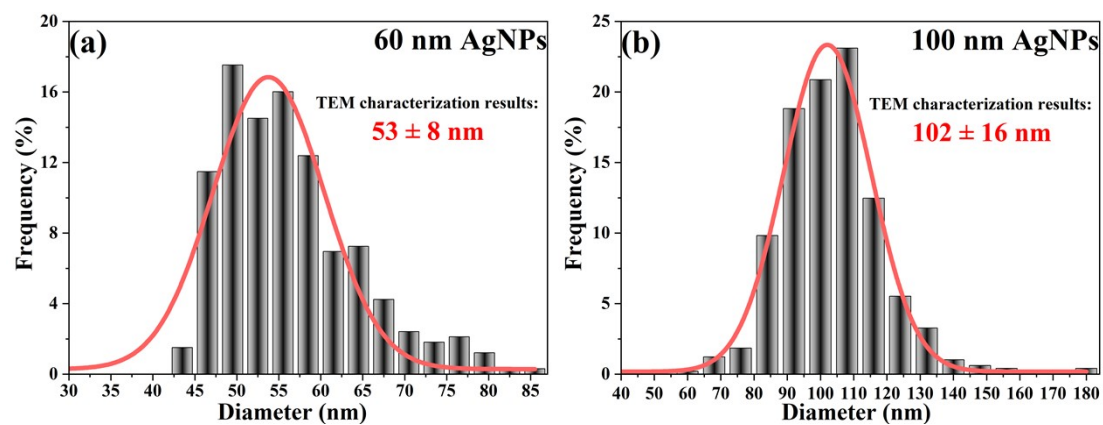


Figure S4. Diameter characterization results of (a) 60 nm and (b) 100 nm Ag NPs using transmission electron microscope (TEM).

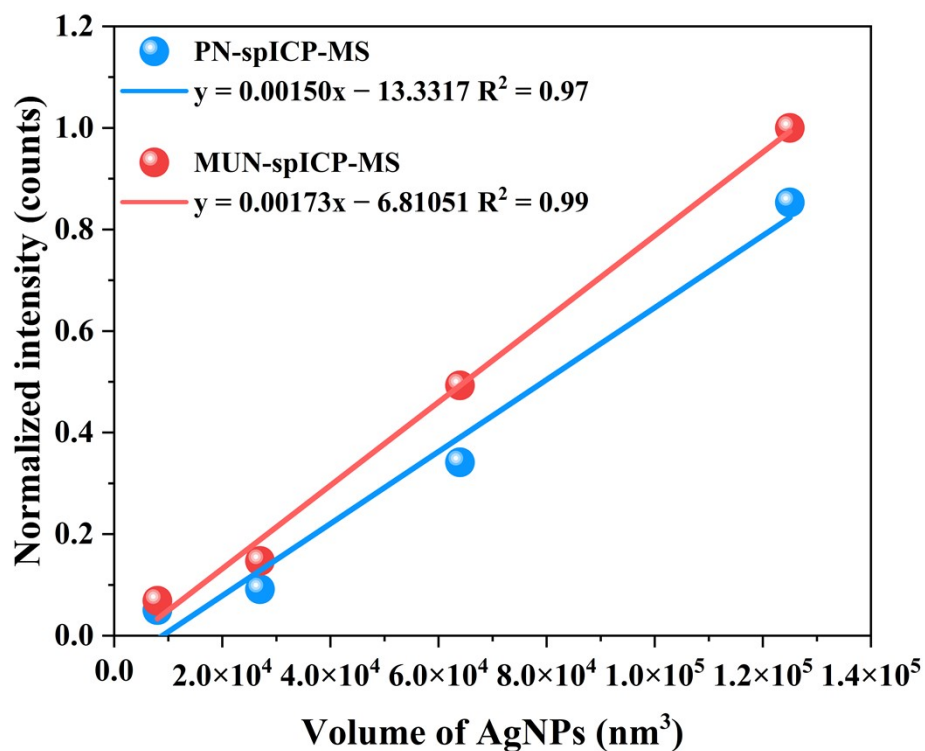


Figure S5. Linear correlation analysis between signal intensity and nanoparticle volume for Ag NPs of various sizes, comparing MUN-spICP-MS (red line) and PN-spICP-MS (blue line). The horizontal axis represents nanoparticle volume calculated from NPs diameters, while the vertical axis represents the average signal intensity of NP pulse signals collected over 5 minutes. All intensities were normalized to the maximum value.

Table S1. The driven power of the MUN system at different sample uptake flow rates.

The driven power of MUN (W)	The sample uptake flow rate ($\mu\text{L min}^{-1}$)
0.05	10
0.06	15
0.08	20
0.10	25
0.11	30
0.14	40
0.17	50
0.20	60

Table S2. The TE of MUN-spICP-MS at different sample uptake flow rates.

Sample uptake flow rates ($\mu\text{L min}^{-1}$)	Particle number concentration (mL^{-1})	Acquisition time (s)	NP number (particles)	Detected pulses events	TE (%)
10	8×10^4	60	800	641	80
15	8×10^4	60	1200	972	81
20	8×10^4	60	1600	1296	81
25	8×10^4	60	2000	1562	78
30	8×10^4	60	2400	1533	64
40	8×10^4	60	3200	1121	35
50	8×10^4	60	4000	762	19
60	8×10^4	60	4800	339	7

Table S3. The comparison between measured diameters of Ag NPs using MUN-sp-ICPMS, PN-spICP-MS, TEM, alongside the nominal values provided by the supplier.

	60 nm Ag NPs	100 nm Ag NPs
Nominal values	60 ± 8 nm	100 ± 8 nm
MUN-spICP-MS	54 ± 9 nm	96 ± 10 nm
PN-spICP-MS	57 ± 2 nm	93 ± 7 nm
TEM	53 ± 8 nm	102 ± 16 nm